RNA (2002), *8*:150–165. Cambridge University Press. Printed in the USA.

DOI: 10.1017.S1355838201010020

Saccharomyces cerevisiae nucleolar protein Nop7p is necessary for biogenesis of 60S ribosomal subunits

CYNTHIA C. ADAMS,* JELENA JAKOVLJEVIC,* JUDIBELLE ROMAN, PIYANUN HARNPICHARNCHAI, and JOHN L. WOOLFORD, JR.

Department of Biological Sciences, Carnegie Mellon University, Pittsburgh, Pennsylvania 15213, USA

ABSTRACT

To identify new gene products that participate in ribosome biogenesis, we carried out a screen for mutations that result in lethality in combination with mutations in *DRS1*, a *Saccharomyces cerevisiae* nucleolar DEAD-box protein required for synthesis of 60S ribosomal subunits. We identified the gene *N0P7* that encodes an essential protein. The temperature-sensitive *nop7-1* mutation or metabolic depletion of Nop7p results in a deficiency of 60S ribosomal subunits and accumulation of halfmer polyribosomes. Analysis of pre-rRNA processing indicates that *nop7* mutants exhibit a delay in processing of 27S pre-rRNA to mature 25S rRNA and decreased accumulation of 25S rRNA. Thus Nop7p, like Drs1p, is required for essential steps leading to synthesis of 60S ribosomal subunits. In addition, inactivation or depletion of Nop7p also affects processing at the A_0, A_1, and A_2 sites, which may result from the association of Nop7p with 35S pre-rRNA in 90S pre-rRNPs. Nop7p is localized primarily in the nucleolus, where most steps in ribosome assembly occur. Nop7p is homologous to the zebrafish *pescadillo* protein necessary for embryonic development. The Nop7 protein contains the BRCT motif, a protein–protein interaction domain through which, for example, the human BRCA1 protein interacts with RNA helicase A.

Keywords: BRCT motif; DEAD-box proteins; nucleolus; ribosome biogenesis; synthetic lethality; yeast

INTRODUCTION

Ribosomal RNA processing and ribosome assembly have been studied in many different eukaryotes (reviewed in Eichler & Craig, 1994), but have been best characterized in the yeast *Saccharomyces cerevisiae* (reviewed in Kressler et al., 1999; Venema & Tollervey, 1999). The yeast ribosome consists of the 40S subunit, which contains the 18S rRNA and 33 different proteins, and the 60S subunit, which contains the 25S, 5.8S, and 5S rRNAs and 46 different proteins. The 18S, 5.8S, and 25S rRNAs are transcribed by RNA polymerase I as a single 35S precursor, whereas 5S rRNA is transcribed independently from separate genes by RNA polymerase III. The 35S rRNA precursor undergoes sequential endo- and exonucleolytic cleavages to generate the mature rRNAs. Concomitant with its synthesis and processing, rRNA is covalently modified by methylation and pseudouridylation and assembles with ribosomal proteins to form mature 40S and 60S ribosomal subunits. These concerted pathways of rRNA processing and ribosome assembly require a number of nonribosomal *trans*-acting factors, including more than 100 small RNAs and at least 70 different proteins (Kressler et al., 1999; Venema & Tollervey, 1999). The majority of these molecules reside in the nucleolus, the nuclear subcompartment where most of the steps in ribosome biogenesis occur.

An important class of nucleolar proteins necessary for ribosome biogenesis is the DEAD-box family of putative RNA helicases (Fuller-Pace, 1994; de la Cruz et al., 1999). Seventeen different DEAD-box proteins (DBPs) have been implicated in biogenesis of yeast ribosomes. The precise functions of these nucleolar DBPs are not known, but might include rearranging RNA structure to provide access to nucleases, catalyzing association or dissociation of snoRNAs and rRNAs, or altering conformation of nucleolar RNA, protein, or RNP complexes to permit association or dissociation of other assembly factors or ribosomal proteins (reviewed in Schwer, 2001; Tanner & Linder, 2001). Nucleolar DBPs might function in multiprotein complexes, as has been shown for several other helicases involved in

Reprint requests to: John L. Woolford, Jr., Department of Biological Sciences, Carnegie Mellon University, 616 Mellon Institute, 4400 Fifth Avenue, Pittsburgh, Pennsylvania 15213, USA; e-mail: jw17@andrew.cmu.edu.

*These authors contributed equally to this work.

mRNA processing or turnover (Margossian et al., 1996; Mitchell et al., 1997; Vanzo et al., 1998). The partners of these helicases include proteins that stimulate helicase activity of the DBPs and nucleases that may require the helicases to alter RNA secondary structure prior to degradation. Therefore, to understand the function of nucleolar DBPs, it is important to identify their protein partners.

We previously identified the nucleolar DBP Drs1p, which is necessary for biogenesis of the 60S ribosomal subunit (Ripmaster et al., 1992). To identify other molecules that function together with Drs1p, we carried out a genetic screen for mutations that are synthetically lethal with *drs1* mutations. Such synthetic lethal screens have been especially useful in studies of pathways of RNA processing (Frank et al., 1992; Liao et al., 1993; Bergès et al., 1994; Simos et al., 1996; Venema & Tollervey, 1996; Venema et al., 1997; Xu et al., 1998) or in studies of multimolecular complexes (Fabre et al., 1994; Doye & Hurt, 1995). Our screen led to the isolation of three genes whose protein products play a role in ribosome biogenesis, and thus may functionally interact with Drs1p. In this report, we describe one of these genes, *NOP7*. We show that Nop7p is an essential, conserved protein located in the nucleolus. The *nop7-1* mutation or depletion of Nop7p results in a deficiency of 60S ribosomal subunits, a kinetic delay in processing of 27S pre-rRNAs to 25S rRNA, and a decrease in 25S rRNA. Interestingly, Nop7p contains a BRCT motif thought to function in other proteins as a structural domain for protein–protein interactions, including interactions with an RNA helicase (Anderson et al., 1998; Zhang et al., 1998).

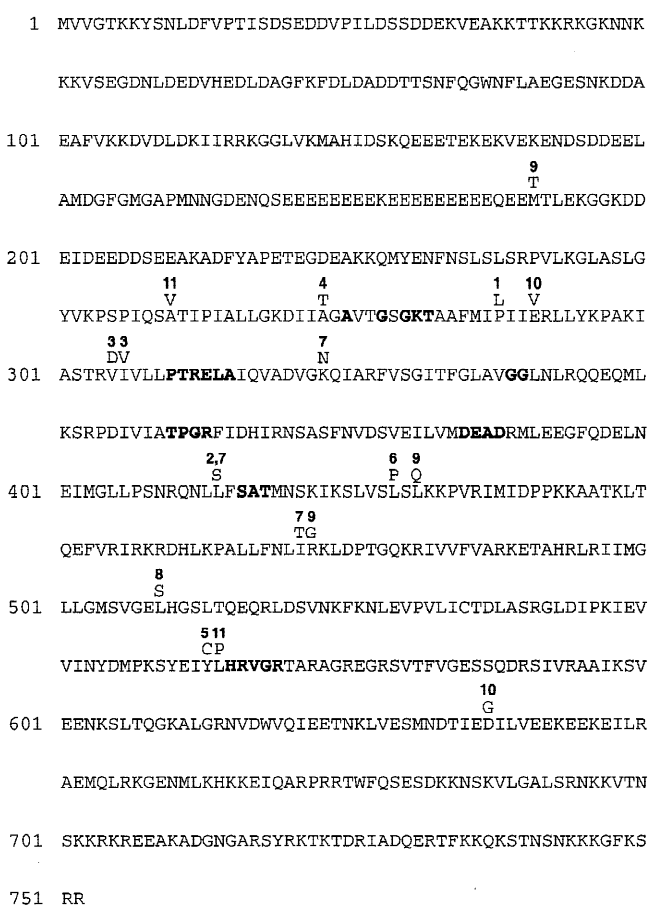

FIGURE 1. Mutant alleles of *DRS1*. Amino acids changed in each of the 10 new mutant alleles of *DRS1*, plus the original *drs1-1* mutation, are indicated in single-letter code above each altered amino acid. The *drs1* allele number is indicated above the mutated amino acid. Each of the conserved motifs present in the core helicase domains of the DEAD-box family is indicated in bold face.

RESULTS

Screen for mutations synthetically lethal with mutations in the nucleolar DEAD-box protein Drs1p

We expected that the spectrum of mutations that would cause lethality in combination with a *drs1* mutation would depend upon the particular mutant allele of *drs1*. Previously, we had identified one mutant allele of *DRS1*, *drs1-1*. Therefore, to increase the likelihood of identifying different gene products interacting with Drs1p, we first isolated additional *drs1* mutants. PCR mutagenesis and gap repair in vivo were used to generate mutations in *DRS1*, screening for cold-sensitive (Cs^-) or temperature-sensitive (Ts^-) conditional lethal mutant strains. We identified the *drs1-2–drs1-11* mutants, all of which are cold-sensitive for growth at 13 °C. Six of these mutants contain single mutations in *DRS1*, and the remaining four contain two or more mutations in *DRS1* (Fig. 1). All of the mutations lie within the central core domain of *DRS1* containing the conserved motifs of the DEAD-box family (de la Cruz et al., 1999). Although none of the mutations change any of the highly conserved amino acids, several alter amino acids immediately adjacent to the GKT, PTRELA, SAT, or HRVGR motifs. Each *drs1* mutant is deficient in 60S ribosomal subunits and accumulates halfmer polyribosomes (data not shown). Pulse-chase analysis was performed to analyze rRNA processing in the *drs1-5* and *drs1-11* mutants. As observed for the *drs1-1* mutant, both the *drs1-5* and *drs1-11* mutants accumulate the 27SB pre-rRNA after 60 min at 13 °C, fail to produce additional 25S rRNA, but generate wild-type levels of 18S rRNA, consistent with a specific defect in biogenesis of 60S ribosomal subunits (Fig. 2 and data not shown).

To screen for mutations lethal in combination with *drs1* mutations, we constructed *ade2 ade3 leu2 ura3 drs1*Δ haploid yeast containing a *CEN URA3 ADE3 DRS1* plasmid and a *CEN LEU2* plasmid bearing either *drs1-2* or *drs1-5*. We specifically chose the *drs1-2* and *drs1-5* alleles because they contain single mutations near two different conserved DBP motifs. *drs1-2* contains a Leu414Ser mutation adjacent to the SAT motif,

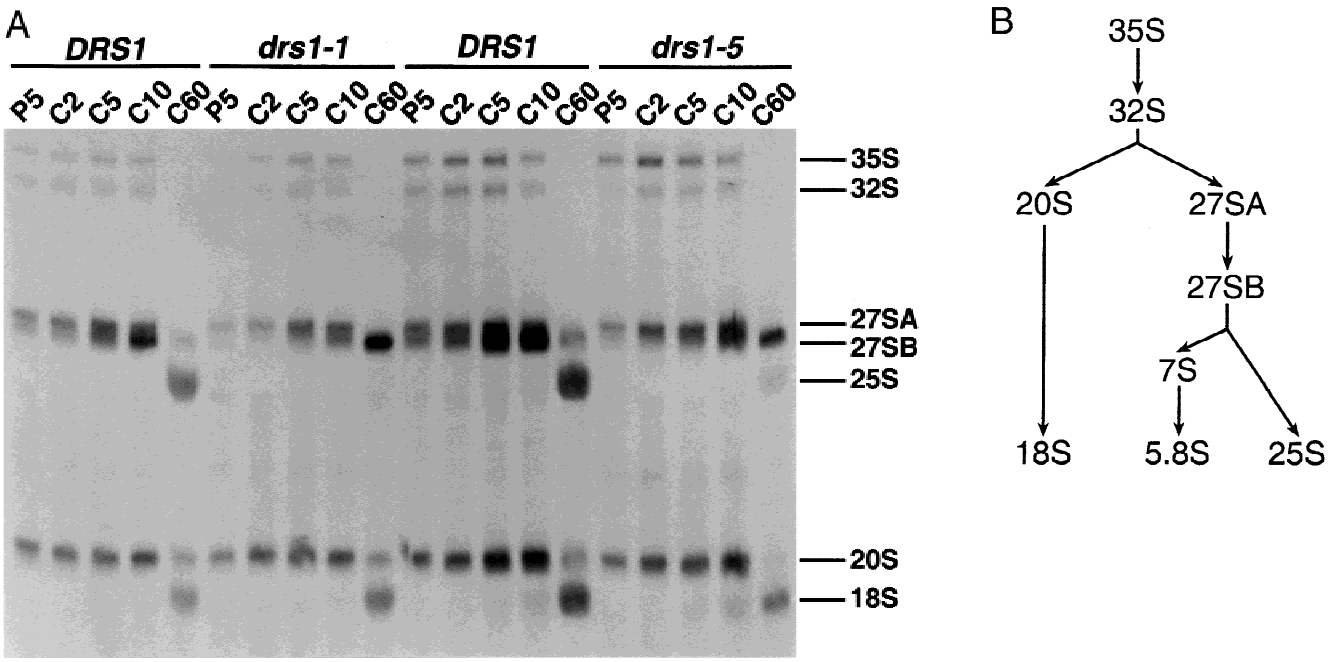

FIGURE 2. **A**: 27SB pre-rRNA accumulates and 25S rRNA is not produced in *drs1-1* and *drs1-5* cold-sensitive mutants. Synthesis, processing, and accumulation of large molecular weight rRNA processing intermediates and products were assayed in the *drs1-1* and *drs1-5* mutants (lanes 6–10 and 16–20, respectively) or in the wild-type *DRS1* strain (lanes 1–5 and 11–15) grown at 30 °C in YEPGlu and shifted to 13 °C for 5 h. Cells were pulse-labeled with [methyl-^{3}H]-methionine for 5 min and chased with excess cold methionine for 2, 5, 10, and 60 min. RNA was extracted and analyzed as described in Materials and Methods. The rRNA primary transcript (35S), processing intermediates (32S, 27SA, 27SB, 20S), and products (18S, 25S) are labeled. Identical results were obtained with *drs1-11* (data not shown). We reproducibly observed slightly slower rates of processing of all rRNAs in the wild-type strains shifted to 13 °C compared to those grown at 30 °C. **B**: Simplified scheme for steps in processing of rRNA.

and *drs1-5* contains a Tyr563Cys mutation near the HRVGR motif. After mutagenesis, nonsectoring 5-FOA^s colonies were identified that contained a chromosomal mutation causing the *DRS1* plasmid to be essential. One dominant synthetic lethal mutation (SL1) was isolated using the *drs1-2* strain and two recessive synthetic lethal mutations (sl2 and sl3) were isolated using the *drs1-5* strain. Each synthetic lethal mutant strain was Ts$^-$ for growth at 37 °C. In crosses of either recessive sl2 or sl3 mutant to a wild-type strain, the Sl$^-$ and the Ts$^-$ phenotypes co-segregated 2$^+$:2$^-$, indicating that each mutant contains a single mutation in a nuclear gene responsible for both the Sl$^-$ and the Ts$^-$ phenotypes. Complementation was observed when strains bearing the two recessive mutations sl2 and sl3 were mated to each other; therefore sl2 and sl3 represent mutations in distinct genes.

To determine whether these synthetic lethal phenotypes were allele specific, we introduced plasmids carrying each of the 11 different *drs1* mutant alleles into each synthetic lethal mutant strain. Whereas SL1 was lethal in combination with all alleles of *DRS1* tested (data not shown), sl2 and sl3 displayed allele specificity. sl2 was lethal only in combination with *drs1-3*, *drs1-5*, *drs1-10*, and *drs1-11* (data not shown), and sl3 was lethal with *drs1-3*, *drs1-5*, and *drs1-11* but not with the other *drs1* mutant alleles (Fig. 3). Further characterization of sl3 and the gene defined by this mutation is described below.

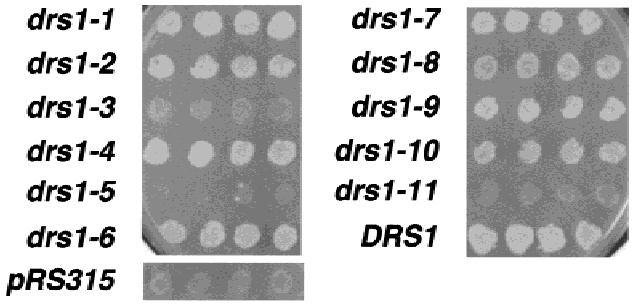

FIGURE 3. The *nop7-1* mutation causes lethality only in combination with *drs1-3*, *drs1-5*, or *drs1-11* mutant alleles. Yeast strain JWY5464 (*drs1Δ ade-2-1 ade3::hisG ura3-1 leu-2-3,112 nop7-1* plus plasmid pJW3956 bearing *URA3*, *ADE3*, *CEN* and *DRS1*) was transformed with *CEN LEU2* plasmid vector pRS315 or pRS315 bearing each of the *drs1* alleles *drs1-1* through *drs1-11*, wild-type *DRS1*, or "empty" vector. Four independent transformants bearing each plasmid were replica-plated to C-leu medium containing 1 mg/mL 5-FOA, as shown. Cells that could not grow on these 5 FOA-containing plates (the *drs1-3*, *drs-5*, and *drs1-11* strains) are unable to lose the *URA3 ADE3 DRS1* plasmid, indicating that the *nop7-1* mutation is lethal in combination with the specific plasmid-borne *drs1* mutant allele. Likewise, the strain carrying the empty vector pRS315 cannot lose the *DRS1* plasmid.

NOP7 encodes a novel, essential protein

Transformation of a yeast genomic library into the sl3 mutant and complementation of its synthetic lethal phenotype yielded ORF YGR103w. Subsequent subcloning, mutagenesis, and linkage analysis demonstrated that YGR103w corresponds to the gene defined by the sl3 mutation (see Materials and Methods). We named this gene *NOP7*, for nucleolar protein 7 (see below), and designated the sl3 mutation *nop7-1*.

To determine whether *NOP7* is an essential gene, we used a one-step PCR strategy to precisely replace one copy of the wild-type *NOP7* open reading frame with the deletion-insertion allele *nop7*Δ::*HIS3*, in diploid strain JWY1401 homozygous for the *his3*-Δ*200* deletion (Baudin et al., 1993). Genomic southern blotting demonstrated that the expected gene replacement had occurred. Upon sporulation of the *nop7*Δ::*HIS3*/*NOP7* diploid and dissection of tetrads, two viable His^- spores and no viable His^+ spores were recovered in each of 20 tetrads (data not shown). The diploid was transformed with a *CEN* plasmid bearing *NOP7* and *LEU2*. Upon sporulation and tetrad dissection, His^+ spores were recovered and were always Leu^+ (data not shown). Thus *NOP7* is an essential gene.

Inactivation or depletion of Nop7p results in a deficiency of 60S ribosomal subunits

To investigate whether Nop7p is essential for production of ribosomes, we assayed the amounts of ribosomal subunits, 80S monoribosomes, and polyribosomes in extracts prepared from the *nop7-1* Ts^- mutant grown at 23 ° and shifted from 23 °C to 37 °C for 5 h. We also assayed ribosome production in a *GAL-NOP7* strain metabolically depleted of Nop7p. In this strain, the chromosomal copy of *NOP7* was disrupted and wild-type *NOP7*, under the control of a *GAL* promoter, was supplied on a plasmid. This strain grew in solid or liquid YEPGal at the same rate as a wild-type *NOP7* strain (Fig. 4A,B), indicating that the *GAL-NOP7* construct is fully functional. However, the *GAL-NOP7* strain did not form colonies on YEPGlu solid medium

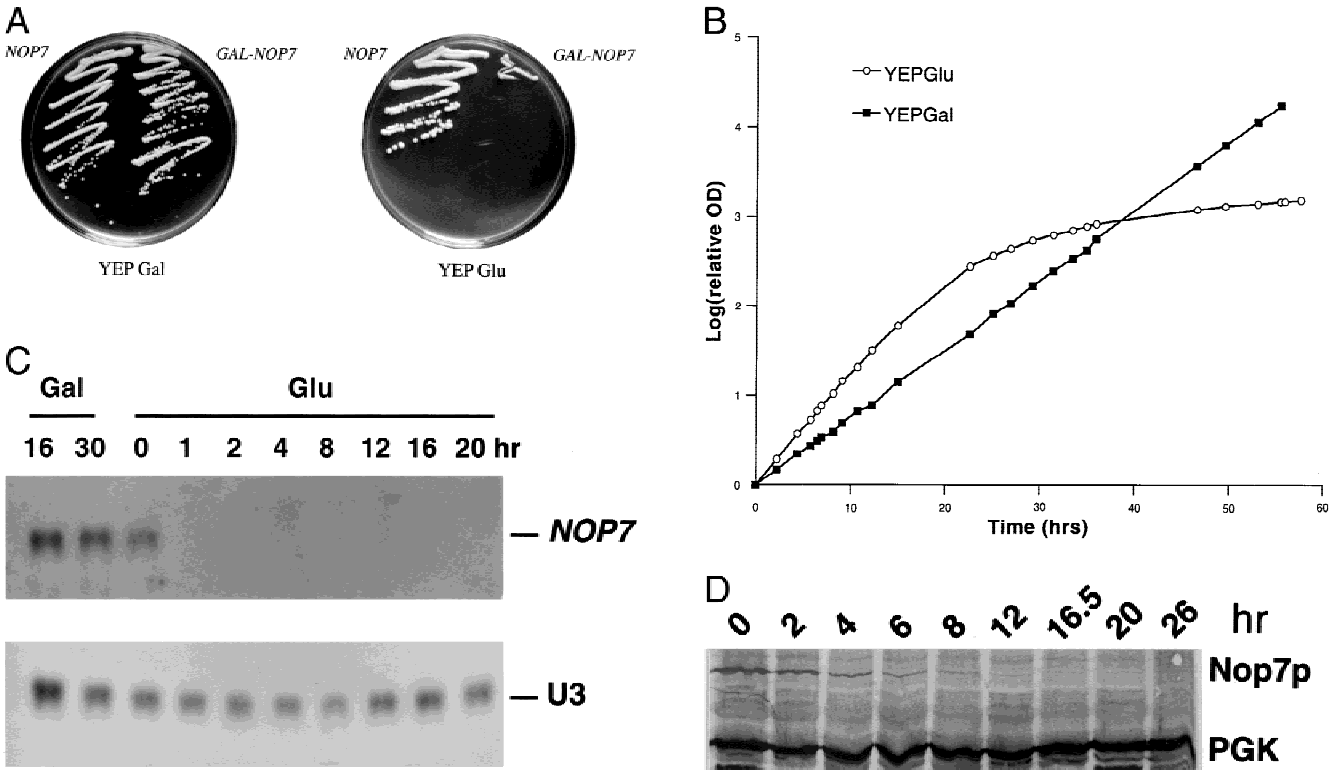

FIGURE 4. Growth of yeast cells is impaired upon depletion of Nop7p. **A**: Yeast strains JWY5853 (*nop7*Δ*::HIS3* plus pRS315 containing *NOP7*) and JWY6901 (*nop7*Δ*::HIS3* plus pBM258T containing *GAL-NOP7*) were streaked on YEPGal or YEPGlu medium and incubated for 4 days at 30 °C. **B**: Liquid growth curve of *GAL-NOP7* strain JWY6901 grown in YEPGal or after shifting to YEPGlu medium. OD_{600} values are plotted as $\log[OD_t/OD_{t0}]$, where OD_{t0} is the initial OD_{600} reading at time 0 before shifting from YEPGal to YEPGlu and OD_t is the OD at time *t* after the shift. Cell cultures were kept at OD_{600} from 0.2–0.8 to maintain logarithmic phase growth. **C**: *NOP7* mRNA is depleted upon shifting the *GAL-NOP7* JWY6901 strain from YEPGal to YEPGlu medium. *NOP7* mRNA was assayed by northern blotting using ^{32}P-labeled *NOP7* ORF as a probe. U3 snoRNA was used as a loading control. **D**: Nop7p is depleted upon shifting the *GAL-NOP7* strain JWY6901 from YEPGal to YEPGlu medium. Rabbit polyclonal antibodies against a peptide from Nop7p were used to assay Nop7p. Yeast PGK was the loading control, assayed using rabbit antibodies.

(Fig. 4A) and exhibited a decreased growth rate in liquid media 24 h after shifting from YEPGal to YEPGlu (Fig. 4B). *NOP7* mRNA was no longer detectable 1 h after the media shift (Fig. 4C) and Nop7 protein was not detectable by 12 h after the shift (Fig. 4D). The *nop7-1* strain grown at 23 °C exhibited a wild-type ribosome profile (Fig. 5A). Likewise, both the wild-type *NOP7* strain and the *GAL-NOP7* strain exhibited wild-type polyribosome profiles after growth in galactose-containing medium (Fig. 5B). However, 5 h after shifting the *nop7-1* strain from 23 °C to 37 °C, and 4 h or 14 h after shifting the *GAL-NOP7* strain from YEPGal to YEPGlu, the num-

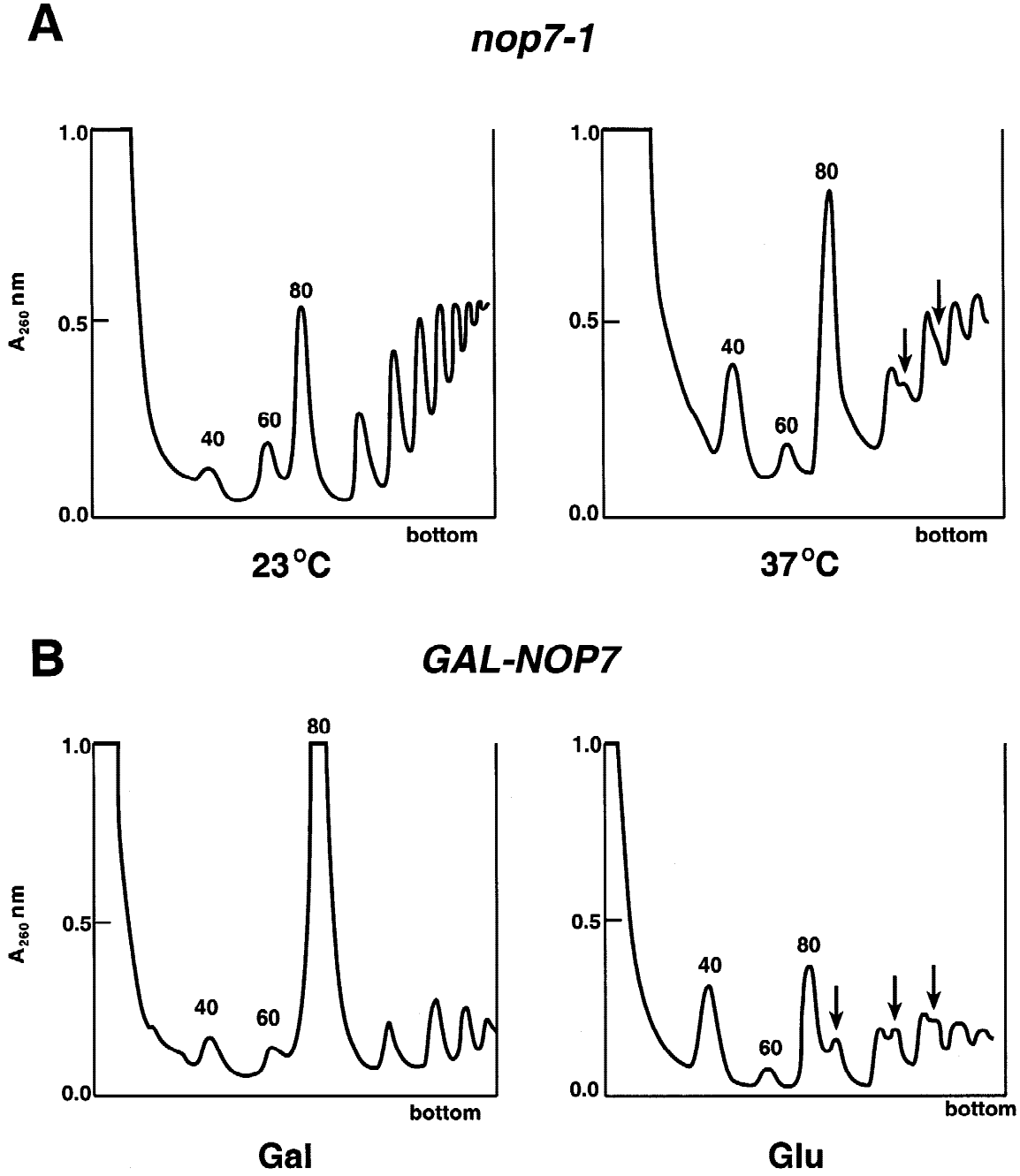

FIGURE 5. The *nop7-1* mutation and depletion of Nop7p result in a deficiency of free 60S ribosomal subunits and accumulation of halfmer polyribosomes. **A**: Extracts were prepared from the *nop7-1* strain JWY5464 grown in YEPGlu at 23 °C to $4 \cdot 10^7$ cells/mL (left), or grown at 23 °C to $3 \cdot 10^7$ cells/mL and shifted to 37 °C for 5 h (right). Cell lysates containing ribosomes and polyribosomes were separated by centrifugation on 7% to 47% sucrose velocity gradients. Peaks representing free 40S and 60S ribosomal subunits and 80S monosomes are labeled. Fractions containing halfmer polyribosomes are indicated by vertical arrows. **B**: The *GAL-NOP7* strain JWY6901 was grown in YEPGal at 30 °C to $5 \cdot 10^7$ cells/mL (left) and shifted to YEPGlu at 30 °C for 14 h (right). Ribosomes and polyribosomes were resolved as described above.

ber of free 60S ribosomal subunits relative to free 40S ribosomal subunits decreased and halfmer polyribosomes accumulated (Fig. 5 and data not shown). The effect on ribosome production in the *GAL-NOP7* strain was greater 14 h after the shift than 4 h, consistent with the observation that Nop7p is only completely depleted by 12 or more hours after the shift.

The peaks of halfmer polyribosomes observed in the *nop7* mutants contain mRNAs associated with integral numbers of ribosomes plus a 43S preinitiation complex, stalled at the AUG initiator codon (Helser et al., 1981; Rotenberg et al., 1988). Such halfmers accumulate when translation initiation is blocked at the 60S subunit joining step (Kang & Hershey, 1994; Eisinger et al., 1997), or when 60S ribosomal subunit assembly is blocked (Rotenberg et al., 1988; Moritz et al., 1990, 1991; Ripmaster et al., 1992, 1993; Deshmukh et al., 1993; Sun & Woolford, 1994; Hong et al., 1997; Vilardell & Warner, 1997; Weaver et al., 1997; Zanchin et al., 1997; Daugeron & Linder, 1998; de la Cruz et al., 1998a, 1998b; Kressler et al., 1998; Ho & Johnson, 1999). The accumulation of halfmers in the *nop7* mutants most likely resulted from a block in 60S ribosomal subunit assembly, as the peak of free 60S ribosomal subunits was reduced in the *nop7-1* mutant or upon depletion of Nop7p. We confirmed that there is a deficit of 60S ribosomal subunits upon depletion of Nop7p, by quantifying total ribosomal subunits from extracts subjected to centrifugation on high salt sucrose gradients. The ratio of 60S subunits to 40S subunits monitored by absorbance at 254 nM was 2.4 in wild-type strains compared to 1.3 in the Nop7p-depleted strain (data not shown). Taken together, these results indicate that inactivation or depletion of Nop7p affects the assembly of ribosomes rather than their function. These effects on 60S ribosomal subunits most likely are a direct result of inactivation or depletion of Nop7p, rather than being an indirect result of impaired growth rate. The 60S ribosomal subunits were decreased before any discernible decrease in the rate of division of the *nop7-1* or *GAL-NOP7* strains.

Nop7p is a nucleolar protein

Most steps in ribosome biogenesis occur in the nucleolus, whereas ribosome function occurs in the cytoplasm. Therefore, to distinguish further whether Nop7p is required for the assembly versus the function of 60S ribosomal subunits, we determined the subcellular localization of Nop7p. To do so, we constructed strain JWY6700 in which the only functional Nop7p protein contains a triple HA epitope tag near its carboxyl terminus. This strain grew at the same rate as a control strain containing untagged wild-type *NOP7* (data not shown), indicating that the HA-tagged Nop7p is functional. Western immunoblotting demonstrated that a polypeptide of the expected size was present in the *HA-NOP7* strain, but not in the untagged *NOP7* strain (data not shown). Indirect immunofluorescence microscopy demonstrated that HA-tagged Nop7p is localized to a crescent- or cap-shaped region largely distinct from the DAPI-stained DNA in the nucleoplasm (Fig. 6). A small amount of Nop7p is reproducibly observed in the nucleoplasm. Thus Nop7p is located within the nucleolus of yeast where ribosomes are assembled, rather than in the cytoplasm, where ribosomes function in protein synthesis. This result indicates that Nop7p most likely is a nonribosomal factor necessary for biogenesis of 60S subunits, rather than a component of mature ribosomes.

Processing of 27S pre-rRNA is delayed and production of 25S rRNA is decreased in *nop7* mutants

To characterize in more detail the role of Nop7p in the production of 60S ribosomal subunits, we assayed rRNA processing in the *nop7-1* mutant and upon depletion of Nop7p in the *GAL-NOP7* strain. We did so using pulse-chase labeling experiments with [methyl-^{3}H]-methionine and [5,6-^{3}H]-uracil, and by steady-state measurements via northern hybridization and primer extension. The *nop7-1* mutant strain and the *NOP7* wild-type strain grown overnight at 23 °C were shifted to 37 °C for 2 h and pulse-labeled for 5 min with [methyl-^{3}H]-methionine, then chased with an excess of cold methionine for 2, 5, 10, and 60 min. In the wild-type *NOP7* strain, most of the 27SA precursors were converted to 27SB pre-rRNAs after the 5-min pulse, and little 27SA or 27SB precursors remained by the 5-min chase (Fig. 7A). In contrast, the *nop7-1* mutant exhibited a greater amount of 27SA precursor than 27SB precursor after the 5-min pulse. Significant amounts of both of these precursors were detected after the 2-min chase, and more 27SB precursor RNA was present after the 5-min chase than in the *NOP7* strain (Fig. 7A). By the 60-min chase point, substantially less 25S rRNA accumulated relative to 18S rRNA in the *nop7-1* strain compared to the *NOP7* strain. The decreased production of 25S rRNA relative to 18S rRNA was quantified by direct measurement of the radioactivity in these RNAs. The ratio of 25S to 18S rRNA in the *nop7-1* mutant 60 min after the chase was 0.89, compared to a ratio of 2.02 in the wild-type *NOP7* strain. We also observed a small amount of 35S and 32S pre-rRNA at the 2-min chase point in the *nop7-1* mutant but not in wild-type *NOP7* strain (Fig. 7A, compare lanes 1 and 2 with lanes 6 and 7). There was no difference in the rate of formation of 18S rRNA from the 20S rRNA intermediate, or in the amount of 18S rRNA produced in the *nop7-1* strain versus the *NOP7* strain (Fig. 7A). Similar results were obtained upon depletion of Nop7p in the *GAL-NOP7* strain (data not shown).

To exclude a defect in rRNA methylation and to assay the synthesis of low molecular weight 5S and 5.8S

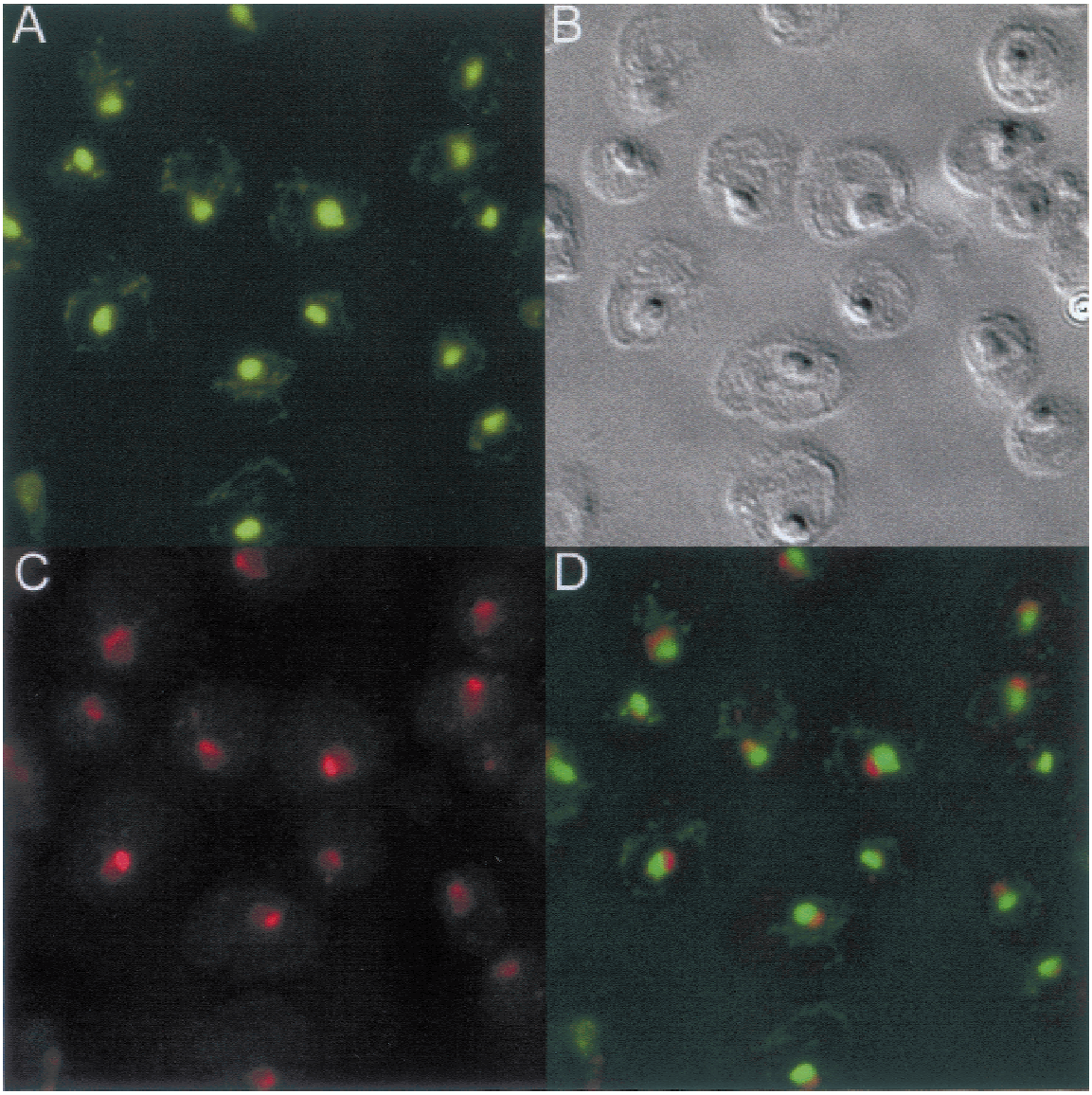

FIGURE 6. HA-tagged Nop7p is localized in the nucleolus. Indirect immunofluorescence microscopy was carried out with strain JWY6700 (*nop7*Δ*::HIS3* plus plasmid pRS315 containing *CEN LEU2* and triple HA-tagged *NOP7*). **A**: DNA was stained with 4′, 6-diamidino-2-phenylindole dihydrochloride (DAPI). **B**: Nomarski image. **C**: HA-Nop7p was detected with mouse monoclonal antibody 16B12 directed against the influenza hemagglutinin epitope, followed by decoration with a rhodamine-conjugated rabbit anti-mouse IgG. **D**: Merged image. Pseudocolors were assigned to the digitized micrographs (red = rhodamine; green = DAPI).

rRNAs and tRNAs, we performed pulse-chase analysis using [5,6-^{3}H]-uracil with *NOP7* and *nop7-1* strains 2 h after shifting from 23 °C to 37 °C, and with *NOP7* and *GAL-NOP7* strains 14 h after shifting from YEPGal to YEPGlu medium. As observed with the [methyl^{-3}H]-methionine pulse-chase experiments, processing of 27S rRNA to 25S rRNA was delayed and 25S rRNA accumulated at lower levels in the *nop7* mutants compared to the wild-type *NOP7* control strains (data not shown). The ratio of 25S to 18S rRNA was 1.14 after the chase in the Nop7p-depleted strain compared to 2.14 for the wild-type *NOP7* strain. Analysis of low molecular weight RNAs indicated that in the Nop7p-depleted strain or the *nop7-1* mutant, there was a slight delay in production of the 7S rRNA processing intermediate derived from the 27SB rRNA, and a slight delay in production of 5.8S rRNA from 7S rRNA (Fig. 7B and data not shown). Synthesis of 5S rRNA and tRNAs was not affected in the *nop7-1* mutant or upon depletion of Nop7p (Fig. 7B and data not shown). The absence of effects on production of 5S rRNA and tRNAs, as well as on methylation of rRNA, indicate that the effects of *nop7* mutants on 27S rRNA processing are specific. The accumulation of newly synthesized 5S rRNA at wild-type levels in *nop7* mutants is consistent with our previous observations that 5S rRNA exists as a stable RNP complex

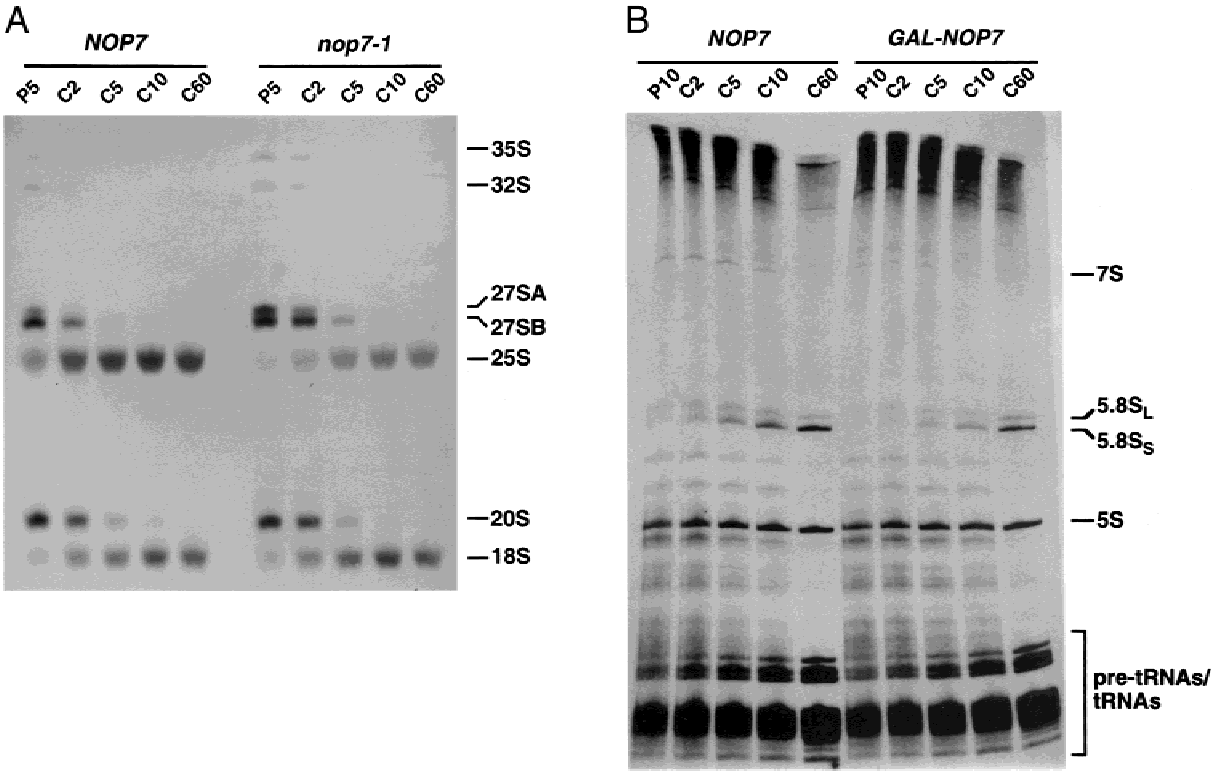

FIGURE 7. The *nop7-1* mutation or depletion of Nop7p delays processing of 27S pre-rRNA to mature 25S rRNA and impairs accumulation of 25S rRNA. **A**: Synthesis, processing, and accumulation of large molecular weight rRNA processing intermediates and products were assayed in the *nop7-1* mutant strain JWY5464 grown at 23 °C in YEPGlu and shifted to 37 °C for 4 h. Cells were pulse-labeled with [methyl-^{3}H]-methionine for 5 min and chased with excess cold methionine for 2, 5, 10, and 60 min. RNA was extracted and analyzed as described in Materials and Methods. The rRNA primary transcript, processing intermediates, and products are labeled. **B**: Production of small molecular weight rRNAs and tRNAs was assayed in the *NOP7* strain JWY5853 and the *GAL-NOP7* strain JWY6901 grown in YEPGal at 30 °C then shifted to YEPGlu for 14 h. Cells were pulse-labeled with [5,6-^{3}H]-uracil for 5 min and chased with excess cold uracil for 2, 5, 10, and 60 min. RNA was extracted and analyzed as described in Materials and Methods. The 7S rRNA intermediate, 5.8S$_L$ and 5.8S$_S$ RNA products, 5S rRNA, and tRNAs are labeled.

with rpL5, independent of ribosomes, which is relatively stable when assembly of 60S ribosomal subunits is disrupted (Moritz et al., 1990; Deshmukh et al., 1993).

To further analyze the steps in pre-rRNA processing that are affected upon depletion of Nop7p, we examined the steady-state levels of rRNA precursors, processing intermediates, and products by northern blotting. To distinguish each rRNA species, oligonucleotide probes were used that are complementary to different portions of the 5′ ETS, ITS1, ITS2, 25S rRNA, and 18S rRNA. RNA was extracted from the *GAL-NOP7* and wild-type *NOP7* strains 0, 4, 19, and 26 h after shifting the cells from YEPGal to YEPGlu. Examination of the blots (Fig. 8) and quantification by phosphorimaging indicated that the amount of 25S rRNA relative to 18S rRNA decreased by 50%, and that levels of 27SA$_3$, 27SA$_2$, and 27SB pre-rRNAs increased 3- to 10-fold. These results suggest that in the absence of Nop7p, processing of the 27S pre-rRNAs is decreased, resulting in diminished amounts of mature 25S rRNA. We also observed increased amounts of the 35S and 32S pre-rRNAs and the aberrant 23S pre-rRNA intermediate upon depletion of Nop7p, consistent with a block in processing at the A$_0$, A$_1$, and A$_2$ sites.

Northern hybridization does not distinguish between the 27SA$_2$ and the 27SA$_3$ precursors, or between the 27SB$_L$ and 27SB$_S$ precursors. To assay levels of these precursors and to determine whether processing at the A$_2$, A$_3$, and B sites was correct at the nucleotide level, primer extension assays were performed using oligonucleotides complementary to sequences 3′ of these sites. Results confirmed that only modest levels of 27S precursors accumulated and that processing occurred precisely at the A$_2$, A$_3$, B$_L$, and B$_S$ sites in ITS1 (data not shown).

DISCUSSION

To identify proteins that function together with Drs1p in the synthesis of 60S ribosomal subunits, we screened for mutations that are lethal in combination with *drs1* mutations. Three mutant strains were identified in which production of 60S ribosomal subunits was compromised. We have characterized in detail the *NOP7* gene

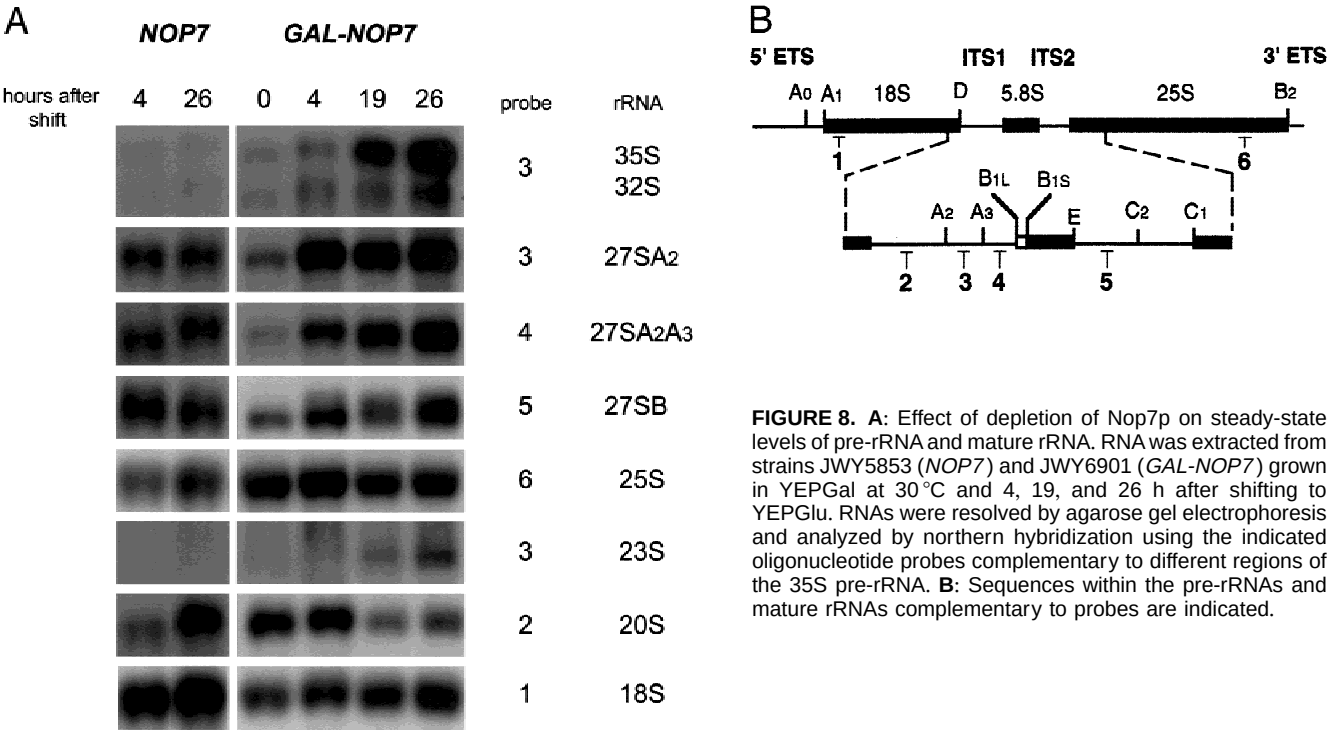

FIGURE 8. **A**: Effect of depletion of Nop7p on steady-state levels of pre-rRNA and mature rRNA. RNA was extracted from strains JWY5853 (*NOP7*) and JWY6901 (*GAL-NOP7*) grown in YEPGal at 30 °C and 4, 19, and 26 h after shifting to YEPGlu. RNAs were resolved by agarose gel electrophoresis and analyzed by northern hybridization using the indicated oligonucleotide probes complementary to different regions of the 35S pre-rRNA. **B**: Sequences within the pre-rRNAs and mature rRNAs complementary to probes are indicated.

corresponding to sl3. *NOP7* is an essential gene encoding a highly conserved protein localized to the nucleolus. Inactivation of Nop7p in the *nop7-1* mutant or depletion of Nop7p using the *GAL-NOP7* conditional expression construct results in a deficit of 60S ribosomal subunits and accumulation of halfmer polyribosomes. Processing of the 27S rRNA precursors is slightly delayed and production of mature 25S rRNA is reduced. However, processing of each rRNA occurs accurately; no aberrant processing intermediates accumulate. These results lead us to conclude that Nop7p, like Drs1p, is an essential nucleolar protein necessary for biogenesis of 60S ribosomal subunits.

Where does Nop7p function in the pathway of 60S ribosomal subunit biogenesis?

Although a few nucleolar proteins have clearly defined functions, such as nucleases, the roles of most nucleolar proteins, including Nop7p, remain unclear. However, a few clues are available from the sequence of the Nop7 protein and from the phenotype of *nop7* mutants. Although Nop7 does not resemble any known nuclease and does not contain any motifs known to recognize RNA, it does contain the BRCT motif first found in the BRCA1 protein (Koonin et al., 1996; Callebaut & Mornon, 1997). This motif can fold into a well-defined structure that may function as a protein–protein interaction domain (Zhang et al., 1998). Consequently, several BRCT-containing proteins are thought to function as scaffolding molecules to hold together components of multimolecular complexes. For example, the human BRCA1 protein interacts with RNA helicase A through its BRCT motif (Anderson et al., 1998). Thus a likely function for Nop7p is to serve as a scaffolding protein to hold together molecules necessary for ribosome assembly or rRNA processing. Consistent with this idea, we have recently found that Nop7p copurifies with 66S preribosomal particles (Harnpicharnchai et al., 2001).

Processing of 27SA and 27SB pre-rRNAs appears to be slowed but not completely blocked in *nop7* mutants. The absence of a strong block in rRNA processing suggests that Nop7p is not directly involved in rRNA processing. It seems more likely that Nop7p helps to establish the proper context of the assembling ribosome, so that rRNA is properly folded for its processing or assembly with other molecules to form a stable, mature 60S subunit. In the absence of Nop7p function, improperly or incompletely assembled 66S preribosomal particles may fall apart and the protein and RNA components of the assembly intermediate might be degraded. However, our pulse-chase and northern data do not allow us to distinguish whether in *nop7* mutants 27S pre-rRNA is degraded so that less 25S, 7S, and 5.8S rRNAs are produced, or 25S, 7S, and 5.8S rRNAs are made in normal amounts, but subsequently degraded. Alternatively, processing of 27S pre-rRNAs to 25S RNA may simply be occurring in proper fashion but at a slower rate in *nop7* mutants. It

is also possible that Nop7p functions in transport of pre-ribosomes from the nucleolus to the nucleoplasm or cytoplasm, rather than in assembly. Mutants defective in ribosome transport often also exhibit defects in assembly, perhaps due to failure to recycle assembly factors (Stage-Zimmerman et al., 2000; Gadal et al., 2001).

The accumulation of 35S and 32S rRNA precursors in the *nop7* mutants suggests that processing at the A_0, A_1, and A_2 sites may be delayed when production of 25S and 5.8S rRNA is altered. Similar effects have been observed in other mutants defective in 60S subunit biogenesis, suggesting that the pathways for biogenesis of the two subunits may interact or may be subject to cross regulatory controls (reviewed in Venema & Tollervey, 1999). Recently we have found that Nop7p is associated with 35S pre-rRNA as well as 27S pre-rRNA, suggesting that Nop7p may first associate with nascent ribosomes in the 90S pre-rRNP before it functions in 66S pre-rRNPs (Harnpicharnchai et al., 2001). Therefore an alternative explanation for the effects on A_0, A_1, and A_2 processing in the *nop7* mutants is that partial loss of Nop7p function might also impact the early steps of pre-rRNA processing by affecting structure or function of 90S pre-rRNPs.

It is not surprising that the small decreases in the rate of production of 25S rRNA and 60S ribosomal subunits that we observe over a period of minutes to several hours in *nop7* mutants can eventually (after 10–20 h) result in cessation of growth. The demands of rapidly growing yeast cells for ribosomes are great; approximately 2,000 ribosomes are synthesized each minute (Warner, 1999). When ribosome assembly is slowed or stopped, the numbers of ribosomes will be diluted by cell division and eventually drop below a threshold necessary for continued cell growth and division. Similar results have been observed for other mutants defective in 60S ribosomal subunit biogenesis (Rotenberg et al., 1988; Daugeron & Linder, 1998; de la Cruz et al., 1998a, 1998b; Kressler et al., 1998; Burger et al., 2000).

What is the nature of interactions between Nop7p and Drs1p?

Nop7p, like Drs1p, is a nucleolar protein necessary for production of 60S ribosomal subunits. However, *nop7* mutants are delayed in processing 27S to 25S rRNAs, whereas *drs1* mutants accumulate 27SB pre-rRNA and produce no detectable 25S rRNA (Fig. 2; Ripmaster et al., 1992). Most combinations of double mutants with 60S subunit deficiencies that we and others have constructed do not result in lethality (J.L. Wolford, Jr., unpubl.; P. Linder, pers. comm.). Therefore we believe that the synthetic lethality observed between a subset of the *drs1* mutations and *nop7-1* reflects specific physical or functional interactions between Drs1p and Nop7p, rather than the cumulative effects of diminished 60S subunits. In support of this view, we have discovered that Drs1p cofractionates with Nop7p in 66S preribosomes (Harnpicharnchai et al., 2001). However, we have found no evidence for direct physical interactions between Nop7p and Drs1p; results of two-hybrid tests were negative.

The allele-specific synthetic lethal phenotypes that are observed between *nop7-1* and the *drs1* mutations may offer some clues to the function of Nop7p or to its interactions with Drs1p. *nop7-1* is lethal in combination with *drs1-3*, *drs1-5*, and *drs1-11*, but not with eight other mutant alleles of *drs1*. Each of the 11 different *drs1* mutations results in a deficiency of 60S ribosomal subunits and accumulation of halfmer polyribosomes. There are only slight variations in the extent of the ribosome deficiency phenotype in each of these mutants. However, there is no obvious correlation between these quantitative effects and synthetic lethality with *nop7-1*. Thus the synthetic lethal phenotypes do not merely reflect a general decrease in *drs1* function. DEAD-box proteins contain eight conserved motifs implicated in ATP binding, ATP hydrolysis, RNA binding, and RNA helicase activity (Fuller-Pace, 1994; de la Cruz et al., 1999). *drs1-3* contains Val305Asp and Ile306Val mutations adjacent to the PTRELA motif, *drs1-5* contains a Tyr563Cys mutation adjacent to the HRVGR motif, and *drs1-11* contains Ala260Val and Leu564Pro mutations, the latter adjacent to the HRVGR motif. The other eight *drs1* mutations are present in different portions of the Drs1 protein, including conserved DBP motifs, but none of these are in the HRVGR motif. The HRVGR motif has been implicated in linking ATP binding and hydrolysis with conformational changes important for helicase or translocase activity of DBPs (Pause & Sonenberg, 1992; Pause et al., 1993, reviewed in Tanner & Linder, 2001). Perhaps Nop7p facilitates the association of RNA with Drs1p or the hydrolysis of ATP by Drs1p.

A function in development for metazoan homologs of Nop7p

Nop7p is a highly conserved protein; homologs are found in zebrafish, *Schizosaccharomyces pombe*, *Caenorhabditis elegans*, *Xenopus laevis*, mouse, and human. The zebrafish homolog *pescadillo* was discovered in a screen for embryonic lethal mutations (Allende et al., 1996; Gaiano et al., 1996). By the third day of embryogenesis in zebrafish *pes* mutants, many different organs and tissues, including the brain, liver, and gut, are underdeveloped, and by day 6, the embryos die. The ribosome deficiency phenotype of yeast *nop7* mutants suggests a molecular basis for the zebrafish *pes* mutant phenotypes. The zebrafish *pescadillo* protein, like its yeast homolog Nop7p, may be required for synthesis of ribosomes. Zebrafish embryos might inherit maternal ribosomes, but could require zygotic expression of ribosomal genes and genes encoding

ribosome assembly factors to synthesize additional ribosomes necessary for late stages of development. A shortage of ribosomes might be especially deleterious to the development of rapidly proliferating tissues such as those affected in *pes* embryos. Analogous situations have been observed during development of *X. laevis* and *Drosophila melanogaster*. In *Xenopus*, expression of genes encoding rRNA, ribosomal proteins, small nucleolar RNAs, and nucleolar proteins is activated during embryogenesis to synthesize sufficient ribosomes for late stages of development (Amaldi, 1982; Pierandrei-Amaldi et al., 1985; Caizergues-Ferrer et al., 1989, 1991). *Xenopus* anucleolate mutants that contain a deletion of most of the cluster of reiterated genes for 18S and 28S rRNAs die at the swimming tadpole stage, due to the inability to make new ribosomes during embryogenesis (Elsdale et al., 1958; Brown & Gurdon, 1964; Wallace & Birnstiel, 1966; Brown & Weber, 1968). *Drosophila minifly*, *Minute*, *mini*, and *bobbed* mutants, which contain mutations in genes encoding a nucleolar protein, a ribosomal protein, 5S rRNA, and 35S rRNA, respectively, have defects in ribosome synthesis that lead to developmental delays and reduction of adult body size (Boncinelli et al., 1972; Procunier & Tartof, 1975; Kay & Jacobs-Lorena, 1985; Giordano et al., 1999). Further studies of Nop7p and other nucleolar molecules will be important not only to understand ribosome biogenesis, but to appreciate complex phenotypes resulting from deficiencies in ribosomes.

MATERIALS AND METHODS

Strains, media, and genetic techniques

Yeast strains used in this study are listed in Table 1. Yeast were grown in YEPGlu, YEPGal, or defined synthetic media and genetically manipulated as described in Sherman et al. (1986). Yeast cells were transformed with DNA using the lithium acetate method (Ito et al., 1983). DNA cloning in *Escherichia coli* and analysis of DNA were performed as described in Sambrook et al. (1989).

Isolation of new mutant alleles of *DRS1*

Mutant alleles of *DRS1* were isolated by PCR mutagenesis and gap repair in vivo, as described in Deshmukh et al. (1995). Plasmid pJW3016 (pRS315 containing *LEU2* plus a *Pst*I-*Xho*I fragment bearing *DRS1*) was digested with *Xba*I and *Bam*HI and the gapped plasmid was purified by gel electrophoresis. DNA from nt −30 to +2092 of the *DRS1* ORF, which includes the coding region for most of the core helicase motifs, was generated by PCR from intact pJW3016, using primers 60A-9 and 60A-6 (Table 2). PCR was carried out under standard conditions, except 10-fold molar less dATP, dGTP, or dTTP was used compared with the other three dNTPs (20 vs. 200 μM). Under these conditions, approximately one to two mutations were generated per 1,000 nt. PCR fragments were co-transformed with the gapped plasmid into yeast strain JWY2181 containing the *drs1::HIS3* null allele and plasmid YEP352-DRSI-HA containing *URA3* and HA-tagged *DRS1.* Plasmid loss assays were performed using 5-fluoroorotic acid (5-FOA) at 13 °C, 30 °C, and 37 °C as described in Deshmukh et al. (1995) to identify strains containing Cs^- or Ts^- alleles of *DRS1* on the *LEU2* plasmid.

Isolation of synthetic lethal mutants

Yeast strains JWY5451, JWY5452, JWY5455, and JWY5456 [*ade2-1 ade3::hisG ura3-1 leu2-3,112* + plasmids pJW3956 (*CEN URA3 ADE3 DRS1*) and either pJW3816 or pJW3828 (*CEN LEU2* and either *drs1-2* or *drs1-5*)] form colonies on YEPGlu medium that exhibit red/white sectoring due to loss of plasmid pJW3956. Each strain was grown in synthetic complete medium lacking leucine and uracil to $5 \cdot 10^7 - 10^8$ cells/mL, plated on YEPGlu solid medium at ~300 colony forming units per plate, and mutagenized to approximately 15% survival with UV irradiation. Alternatively, strains were grown in liquid medium as above, mutagenized to approximately 15% survival with 0.3% EMS, and plated on YEPGlu solid medium as above. Mutagenized cells were incubated at 30 °C for 5–8 days. Approximately 175,000 colonies were screened for a nonsectoring phenotype. Candidates were streaked for single colonies on YEPGlu medium to confirm nonsectoring and plated on medium containing 1 mg/mL 5-FOA to determine whether or not growth depended on the presence of plasmid JW3956 containing *URA3*, *ADE3*, and *DRS1.* Strains retaining pJW3956 for reasons unrelated to synthetic lethality with *drs1-2* or *drs1-5* were identified as follows: the nonsectoring, 5-FOA-sensitive strains were grown in liquid YEPGlu to allow loss of the *CEN LEU2 drs1-2* or *CEN LEU2 drs1-5* plasmid. These Leu^- strains were transformed with pJW3833 (*DRS1 LEU2*), pJW3816 (*drs1-2 LEU2*), or pJW3828 (*drs1-5 LEU2*). Three yeast strains, JWY5459 (SL1), JWY5461 (sl2), and JWY5463 (sl3), in which sectoring was restored when transformed with pJW3833 but was *not* restored when transformed with pJW3816 or pJW3828 were retained as bona fide synthetic lethal mutants.

Cloning and disruption of *NOP7*

The *NOP7* gene defined by the sl3 mutation in JWY5463 was cloned by replacing plasmid pJW3828 (*CEN LEU2 drs1-5*) with plasmid pJW3988 (*CEN LYS2 drs1-5*), generating yeast strain JWY5465. This allowed us to clone *NOP7* from a yeast genomic library cloned in a *CEN LEU2* vector, by transformation of JWY5465 and complementation of the nonsectoring, 5-FOA^s phenotypes. Transformants were selected on complete synthetic medium lacking lysine and leucine, and red/white sectoring 5-FOA^R colonies were identified. Plasmids were extracted from the candidate strains and transformed into *E. coli*. Those plasmids containing *LEU2* (but not *LYS2* or *URA3*) were identified by DNA dot blot analysis and then transformed into yeast strain JWY5465 to reconfirm sectoring and 5-FOA^R phenotypes. The ends of the genomic DNA inserts in each plasmid were sequenced and found to encompass an 8 kb region of chromosome VII containing *MIC1*, YGR101w, YGR102c, YGR103w, and the 3′ end of *SRB5*. To identify which if any of these ORFs complemented the sl3 mutation, several subclones were constructed by mak-

TABLE 1. *S. cerevisiae* strains used in this study.

Strain	Genotype	Source
YCH125	*MATa ade 2-1 ade3::hisG ura3-1 his3-11,15 leu2-3,112 trp1-1 LYS2*	C. Hardy & S. Wente
YCH128	*MATα ade2-1 ade3:hisG ura3-1 his3-11,15 leu2-3,112 TRP1 lys2*	C. Hardy & S. Wente
JWY1401	*MATa/MATα ade2-101/+ can1/+ his3-Δ200/his3-Δ200 leu2-Δ1/leu2-Δ1 lys2-801/lys2-801 trp1-Δ101/ trp1-Δ101 ura3-52/ura3-52*	M. Moritz
JWY5436	*MATa/MATα ade2-1/ade2-1 ade3::hisG/ade3::hisG ura3-1/ura3-1 his3-11,15/his3-11,15 leu2-3,112/ leu2-3,112 trp1-1/TRP1 LYS2/lys2*	YCH125 X YCH128
JWY5439	*MATa/MATα ade2-1/ade2-1 ade3::hisG/ade3::hisG ura3-1/ura3-1 his3-11,15/his3-11,15 leu2-3,112/ leu2-3,112 trp1/TRP1 LYS2/lys2 DRS1/drs1Δ::hisGURA3hisG*	
JWY5440	*MATa/MATα ade2-1/ade2-1 ade3::hisG/ade3::hisG ura3-1/ura3-1 his3-11,15/his3-11,15 leu2-3,112/ leu2-3,112 trp-1/TRP1 LYS2/lys2 DRS1/drs1Δ::hisGURA3hisG*	
JWY5444	*MATa ade2-1 ade3::hisG ura3-1 his3-11,15 leu2-3,112 TRP1 lys2 drs1Δ::hisG* plus pJW3956 (*CEN URA3 ADE3 DRS1)*	
JWY5447	*MATα ade2-1 ade3::hisG ura3-1 his3-11,15 leu2-3, 112 trp1-1 LYS2 drs1Δ::hisG* plus pJW3956	
JWY5451	*MATa ade2-1 ade3::hisG ura3-1 his3-11,15 leu2-3,112 TRP1 lys2 drs1Δ::hisG* plus pJW3956 and pJW3816 (*CEN LEU2 drs1-2*)	
JWY5452	*MATa ade2-1 ade3::hisG ura3-1 his3-11,15 leu2-3,112 TRP1 lys2 drs1Δ::hisG* plus pJW3956 and pJW3828 (*CEN LEU2 drs1-5)*	
JWY5455	*MATα ade2-1 ade3::hisG ura3-1 his3-11,15 leu2-3,112 trp1-1 LYS2 drs1Δ::hisG* plus pJW3956 and pJW3816 (*CEN LEU2 drs1-2)*	
JWY5456	*MATα ade2-1 ade3::hisG ura3-1 his3-11,15 leu2-3,112 trp1-1 LYS2 drs1Δ::hisG* plus pJW3956 and pJW3828 (*CEN LEU2 drs1-5)*	
JWY5459	*MATa ade2-1 ade3::hisG ura3-1 his3-11,15 leu 2-3, 112 TRP1 lys2 drs1Δ::hisG* SL1 plus pJW3956 and pJW3816	
JWY5460	*MATa ade2-1 ade3::hisG ura3-1 his3-11,15 leu2-3,112 TRP1 lys2 drs1Δ::hisG* SL1 plus pJW3956	
JWY5461	*MATa ade2-1 ade3::hisG ura3-1 his3-11,15 leu2-3,112 TRP1 lys2 drs1Δ::hisG* sl2 plus pJW3956 and pJW3828	
JWY5462	*MATa ade2-1 ade3::hisG ura3-1 his3-11,15 leu2-3,112 TRP1 lys2 drs1Δ::hisG* sl2 plus pJW3956	
JWY5463	*MATa ade2-1 ade3::hisG ura3-1 his3-11,15 leu2-3,112 TRP1 lys2 drs1Δ::hisG* sl3 plus pJW3956 and pJW3828	
JWY5464	*MATa ade2-1 ade3::hisG ura3-1 his3-11,15 leu2-3,112 TRP1 lys2 drs1Δ::hisG* sl3 plus pJW3956	
JWY5465	*MATa ade2-1 ade3::hisG ura3-1 his3-11,15 leu2-3,112 TRP1 lys2 drs1Δ::hisG* sl3 plus pJW3956 and pJW3988 (*CEN LYS2 drs1-5)*	
JWY5802	*MATα ade2-1 ade3::hisG ura3-1 his3-11,15 leu2-3,112 trp1-1 LYS2 drs1Δ::hisG NOP7::TRP1 NOP7* plus pJW3956 and pJW3828	
JWY5803	*MATa/MATα ade2-1/ade2-1 ade3::hisG/ade3::hisG ura3-1/ura3-1 his3-11,15/his3-11,15 leu2-3,112/ leu2-3,112 trp1-1/TRP1 LYS2/lys2 drs1Δ::hisG/drs1Δ::hisG sl3/SL3 NOP7/NOP7::TRP1 NOP7*	
JWY5827	*MATa/MATα ade2-101/+ can1/+ his3-Δ200/his3-Δ200 leu2-Δ1/leu2-Δ1 lys2-801/lys2-801 trp1-Δ101/ trp1-Δ101 ura3-52/ura3-52 NOP7/nop7Δ::HIS3*	
JWY5850	*Matα his3Δ-200 leu2-Δ1 lys2-801 trp1-Δ101 ura3-52 nop7::HIS3* plus pJW4915 (*CEN URA3 NOP7)*	
JWY5852	*MATα his3Δ-200 leu2-Δ1 lys2-801 trp1-Δ101 ura3-52 nop7::HIS3* plus pJW4915 (*CEN LEU2 HA-NOP7)*	
JWY5853	*MATα his3Δ-200 leu2-Δ1 lys2-801 trp1-Δ101 ura3-52 nop7::HIS3* plus pJW4913 (*CEN LEU2 NOP7)*	
JWY6901	*MATα his3Δ-200 leu2-Δ1 lys2-801 trp1-Δ101 ura3-52 nop7::HIS3* plus pJW6004 (*CEN URA3 GAL-NOP7)*	
JWY6700	*MATα his3Δ-200 leu2-Δ1 lys2-801 trp1-Δ101 ura3-52 nop7::HIS3* plus pJW5814 (*CEN LEU2 NOP7-HA3*)	

ing internal deletions. Plasmid JW3993 containing a deletion from the *Sph*I site in *MIC1* to the *Sac*II site near the 3′ end of YGR102c still complemented sl3, whereas plasmid JW3992 containing a deletion from the *Sac*II site in YGR102c to the *Hin*dIII site within *SRB5* failed to complement sl3. These results suggested that YGR103w was the ORF complementing sl3. To test this hypothesis, YGR103w (and 500 nt of 5′ and 3′ flanking nontranslated sequences) was amplified by PCR using oligonucleotides 103 Bam up and 103 Bam down (Table 2), digested with *Bam*HI and cloned into the *Bam*HI site of plasmid pJW3982 (*CEN LEU2*) to create pJW3998. This plasmid containing the YGR103w ORF complemented sl3. Thus, ORF YGR103w was determined to be the complementing molecule. To determine that the protein encoded by ORF YGR103w conferred the complementing phenotype, and not an RNA molecule transcribed from sequences 5′ or 3′ to the ORF, a frameshift mutation in YGR103w was constructed by digesting plasmid pJW3993 with *Nsi*I, removing the overhanging 3′ ends with Klenow fragment, and relegating the DNA. The plasmid containing this frameshift mutation between codons 72 and 73 of YGR103w failed to complement sl3.

To confirm that YGR103w corresponds to sl3 and is not an extragenic multicopy suppressor of sl3, we tested whether YGR103w is linked to the sl3 locus. The *Bam*HI fragment containing YGR103w was isolated from pJW3998 and inserted into the *Bam*HI site of yeast integrating plasmid pRS304, containing *TRP1* and no yeast origins of replication.

TABLE 2. Oligonucleotides used in this study.

60A-9	5′-GTGCCTACAACAGCG-3′
60A-6	5′-TTTTGCTGTTAGTGAC-3′
103 Bam Up	5′-AGACGGATCCTTTTACAGCTTCAGCAGA-3′
103 Bam Down	5′-AATTGGATCCCTGCCTTGATGAACTTAA-3′
103 HIS3 pro	5′-CCTGTAGAAAATAGTATAGTAACAGCGGTATCCTACTTATACACTCTTGGCCTCCTCTAG-3′
103 HIS3 term	5′-GAGAGGCTATTGGAAAAGAAGAGAAAACTATTTCTTGGAATCTAGTCGTTCAGAATGACACG-3′
JJHA1	5′-CTTCCGCGGAACAATTTTTTTACAGCTTCAGC-3′
NOP7Up	5′-TACTGGATCCGTGTAGTAAATCCTGCTGGTG-3′
JJHA2	5′-GGAGGCCTTTTCTTGGAATCTAGTTTATTCAG-3′
NOP7Down	5′-TACTGGATCCTATAATCATTGGCACCTGGGC-3′
103 Bam NHA	5′-CTTTTTATTTCTTGGATCCCTAGGATAGATACC-3′
1	5′-CATGGCTTAATCTTTGAGAC-3′
2	5′-GCTCTTTGCTCTTGCC-3′
3	5′-TGTTACCTCTGGGCCC-3′
4	5′-AATTTCCAGTTACGAAAATTCTTGT-3′
5	5′-GGCCAGCAATTTCAAGTTA-3′
6	5′-CTCCGCTTATTGATATGC-3′

This plasmid pJW4909 was linearized and transformed into yeast strain JWY5456 [*MAT*α *trp1-1 LYS2 drs1*Δ::*hisG* + plasmids pJW3956 (*CEN URA3 ADE3 DRS1*) and pJW3828 (*CEN LEU2 drs1-5*)] to create strain JWY5802. Integration at the homologous locus in the genome was confirmed by southern blot analysis. JWY5802 was crossed to JWY5463 (*MATa lys2 TRP1* sl3 plus plasmids pJW3956 and pJW3828) to create diploid JWY5803. This diploid was sporulated, tetrads dissected, and phenotypes assessed to score segregation of relevant markers (Sl^-, i.e., 5-FOA^s, Trp^-, and Ts^-). Tetrad types predicted to occur if the sl3 locus is in fact identical to ORF YGR103w were obtained, rather than the very different pattern of tetrad types predicted if sl3 were not identical to YGR103W. For example, *NOP7 TRP1 NOP7* segregated in opposition to *nop7-1*, as expected if sl3 is YGR103w.

A yeast strain containing a *nop7*Δ*::HIS3* null allele was constructed using PCR by the method of Baudin et al. (1993). Oligonucleotides 103HIS3 pro and 103HIS3 term (Table 2) were used as primers with a *HIS3* template substrate to synthesize an 1,100 bp *HIS3* fragment flanked on the 5′ end with nt −43 to nt −1 of *NOP7* and on the 3′ end with nt +1799 to nt +1845 of *NOP7*. This fragment was transformed into diploid yeast JWY1401, homozygous for the deletion allele *his3-*Δ*200*, with selection for His^+ phenotype. Replacement of one wild-type allele of *NOP7* by the *nop7*Δ*::HIS3* null allele in the transformant JWY5827 was confirmed by genomic southern blotting. The lethal phenotype of *nop7*Δ*::HIS3* was demonstrated by sporulation of JWY5827 and dissection of tetrads.

Construction and analysis of a conditional null *GAL-NOP7* strain

The *NOP7* ORF containing *Bam*HI sites at each end was amplified by PCR using primers NOP7Up and NOP7Down (Table 2). The DNA was digested with *Bam*HI and cloned into the *Bam*HI site downstream of the *GAL* promoter in plasmid pBM258T containing *URA3*, to produce plasmid pJW6004. The resulting *GAL-NOP7* plasmid pJW6004 was transformed into yeast strain JWY5853. Subsequent loss of plasmid pJW4913 (*CEN LEU2 NOP7*) produced yeast strain JWY6901 (*nop7::HIS3* plus plasmid pJW6004 containing *CEN URA3 GAL-NOP7*). Levels of *NOP7* mRNA in JWY6901 grown in YEPGal or shifted to YEPGlu were assayed by northern blotting and hybridization using the *NOP7* ORF as a probe. Levels of Nop7p in JWY6901 grown in YEPGal or shifted from YEPGal to YEPGlu were assayed by western blotting using rabbit antibodies, generated by immunization with synthetic peptide GIKYSETSEADKDVNKSK containing amino acids 522 to 539 of Nop7p, linked to KLH (Alpha Diagnostic International). Rabbit polyclonal antibodies against yeast PGK were a kind gift of Dr. Jeremy Thorner.

Fractionation and characterization of polyribosomes

Yeast strains JWY5464 (*nop7-1*) and JWY5444 (*NOP7*) were grown in YEPGlu at 23 °C overnight to $3 \cdot 10^7$ cells/mL and shifted to YEPGlu at 23 °C or 37 °C for 5 h. JWY6901 (*GAL-NOP7*) and JWY5853 (*NOP7*) were grown in YEPGal at 30 °C to $5 \cdot 10^7$ cells/mL and shifted to YEPGlu at 30 °C for 4 h or 14 h. Extracts were prepared from these strains and ribosomal subunits, ribosomes, and polyribosomes were assayed by sucrose gradient centrifugation, as described previously (Sun & Woolford, 1994). To quantify ratios of total subunits, extracts were prepared as above and subjected to sucrose gradient centrifugation, except that 0.5 M KCl was included instead of 0.15 M NaCl in the lysis buffer and sucrose gradient buffer.

Pulse-chase and northern analysis of rRNA processing

The synthesis, processing, accumulation, and turnover of rRNAs were assayed by pulse-chase analysis as described by Venema et al. (1998), with the following exceptions. Strains JWY5464 (*nop7-1*) and JWY5444 (*NOP7*) grown in YEPGlu at 23 °C to $2 \cdot 10^7$ cells/mL were shifted to YEPGlu at 37 °C for 2 h. Strains JWY6901 (*GAL-NOP7*) and JWY5853 (*NOP7*)

grown in YEPGal at 30 °C to $5 \cdot 10^7$ cells/mL were shifted to YEPGlu at 30 °C for 14 h. Both pairs of strains were pulse-labeled with 33 μCi/mL of [methyl-^{3}H]-methionine or 18 μCi/mL of [5,6-^{3}H]-uracil for 5 min and chased for up to 60 min with excess cold methionine or uracil. RNA was extracted and equal cpm of each sample were subjected to electrophoresis on 1.2% agarose 6% formaldehyde gels or 8% acrylamide 8 M urea gels. RNA was capillary blotted (agarose) or electroblotted (acrylamide) onto Nytran Plus and blots were exposed to BIOMAX MS film (Kodak) using a BIOMAX Transcreen-LE (Kodak) at −80 °C. Nytran filters were aligned with the exposed films, positions of the filters containing the 18S and 25S rRNAs were cut out, and were counted by liquid scintillation.

Northern analysis and primer extension were carried out as described in Venema et al. (1998). Yeast strains JWY5853 and JWY6901 were grown in YEPGal at 30 °C to $5 \cdot 10^7$ cells/mL then shifted to YEPGlu for 4 h, 19 h or 26 h. RNA was extracted, subjected to electrophoresis, and blotted as above. Blots were hybridized with ^{32}P-labeled oligonucleotides #1 to #6, complementary to rRNA, as described by Venema et al. (1998).

Construction of HA-tagged Nop7p

To construct an allele of *NOP7* tagged with 3 HA epitopes at its 3′ end, a *Sac*II-*Stu*I DNA fragment containing the *NOP7* ORF was synthesized by genomic PCR using primers JJHA1 and JJHA2, digested with *Sac*II and *Stu*I, and cloned between the *Sac*II and *Stu*I sites of plasmid pJW5636 (*CEN LEU2* HA3-tag). The resulting plasmid pJW5814 bearing *NOP7-HA3* was transformed into yeast strain JWY5850 [*nop7*Δ*::HIS3* plus pJW4914 (*CEN URA3 NOP7*)]. Transformants were plated on medium containing 5-FOA to select for loss of pJW4914, to generate yeast strain JWY6700 [*nop7*Δ*::HIS3* plus pJW5814 (*CEN LEU2 NOP7-HA3*)].

Indirect immunofluorescence microscopy

Strains JWY6700 (*NOP7-HA3*) and JWY5853 (*NOP7*) were grown in YEPGlu at 30 °C to $5–6 \cdot 10^7$ cells/mL, harvested, and prepared for microscopy as described by Pringle et al. (1989). Mouse monoclonal antibody 16B12 directed against the hemagglutinin epitope YPYDVPDYA was used at 1:100 dilution. The secondary antibody used was rabbit anti-mouse immunoglobulin G conjugated with rhodamine at a dilution of 1:100. DAPI (4′, 6 diamidino-2-phenyl indole dihydrochloride) was used to stain DNA. Slides were viewed using a fluorescence microscope (Carl Zeiss) equipped with a 100× objective. Photographs were taken on a Hamamatsu black-and-white CCD-coupled camera. Digital images were acquired in the program Photoshop (Adobe Systems, Mountain View, California).

ACKNOWLEDGMENTS

We thank Elaine Pinheiro for assistance with the synthetic lethal screen, Chris Hardy and Susan Wente for yeast strains YCH125 and YCH128, Jeremy Thorner for antibodies versus yeast PGK, Adam Linstedt, Tina Lee, and Gregory Fisher for help with the microscopy, and Elizabeth Jones for the *LEU2 CEN* yeast genomic library. Thanks to Frances McFarland and Carol Woolford for critical reading of the manuscript and to colleagues in our laboratory for valuable discussions. This study was supported by Public Health Service grants GM28301 from the National Institutes of Health to J.L.W. and GM18708 to J.R. P.H was supported by funds from the government of Thailand.

Received January 4, 2001; returned for revision February 8, 2001; revised manuscript received November 15, 2001

REFERENCES

Allende ML, Amsterdam A, Becker T, Kawakami K, Gaiano N, Hopkins N. 1996. Insertional mutagenesis in zebrafish identifies two novel genes, *pescadillo* and *dead eye*, essential for embryonic development. *Genes & Dev 10*:3141–3155.

Amaldi F. 1982. Expression of ribosomal-protein genes in *Xenopus laevis* development. *Cell 30*:163–171.

Anderson SF, Schlegel BP, Jakajima T, Wolpin ES, Parvin JD. 1998. BRCA1 protein is linked to the RNA polymerase II holoenzyme complex via RNA helicase A. *Nature Genet 19*:254–256.

Baudin A, Ozier KO, Denouel A, Lacroute F, Cullin C. 1993. A simple and efficient method for direct gene deletion in *Saccharomyces cerevisiae*. *Nucleic Acids Res 21*:3329–3330.

Bergès T, Petfalski E, Tollervey D, Hurt EC. 1994. Synthetic lethality with fibrillarin identifies NOP77p, a nucleolar protein required for pre-rRNA processing and modification. *EMBO J 13*:3136–3148.

Boncinelli E, Graziani F, Polito L, Malva C, Ritossa F. 1972. rDNA magnification at the *bobbed* locus of the Y chromosome in *Drosophila melanogaster. Cell Differ 1*:133–142.

Brown DD, Gurdon JB. 1964. Absence of ribosomal RNA synthesis in the anucleolate mutant of *Xenopus laevis*. *Proc Natl Acad Sci USA 51*:139–146.

Brown DD, Weber CS. 1968. Gene linkage by RNA–DNA hybridization. I. Unique DNA sequences homologous to 4S RNA, 5S RNA, and ribosomal RNA. *J Mol Biol 34*:661–680.

Burger F, Daugeron M-C, Linder P. 2000. Dbp10p, a putative RNA helicase from *Saccharomyces cerevisiae*, is required for ribosome biogenesis. *Nucleic Acids Res 28*:2315–2323.

Caizergues-Ferrer M, Mariottini P, Curie C, Lapeyre B, Gas N, Amalric F, Amaldi F. 1989. Nucleolin from *Xenopus laevis*: cDNA cloning and expression during development. *Genes & Dev 3*:324–333.

Caizergues-Ferrer M, Mathieu C, Mariottini P, Amalric F, Amaldi F. 1991. Developmental expression of fibrillarin and U3 snRNA in *Xenopus laevis*. *Development 112*:317–326.

Callebaut I, Mornon JP. 1997. From BRCA1 to RAP1: A widespread BRCT module closely associated with DNA repair. *FEBS Lett 400*:25–30.

Daugeron MC, Linder P. 1998. Dbp7p, a putative ATP-dependent RNA helicase from *Saccharomyces cerevisiae*, is required for 60S ribosomal subunit assembly. *RNA 4*:566–581.

de la Cruz J, Kressler D, Linder P. 1999. Unwinding RNA in *Saccharomyces cerevisiae*: DEAD-box proteins and related families. *Trends Biochem Sci 24*:192–198.

de la Cruz J, Kressler D, Rojo M, Tollervey D, Linder P. 1998a. Spb4p, an essential putative RNA helicase, is required for a late step in the assembly of 60S ribosomal subunits in *Saccharomyces cerevisiae*. *RNA 4*:1268–1281.

de la Cruz J, Kressler D, Tollervey D, Linder P. 1998b. Dob1p (Mtr4p) is a putative ATP-dependent RNA helicase required for the 3′ end formation of 5.8S rRNA in *Saccharomyces cerevisiae*. *EMBO J 17*:1128–1140.

Deshmukh M, Stark J, Yeh L-C, Lee J, Woolford JL Jr. 1995. Multiple regions of yeast ribosomal protein L1 are important for its interaction with 5S rRNa and assembly into ribosomes. *J Biol Chem 270*:30148–30156.

Deshmukh M, Tsay YF, Paulovich AG, Woolford JL Jr. 1993. Yeast ribosomal protein L1 is required for the stability of newly synthesized 5S rRNA and the assembly of 60S ribosomal subunits. *Mol Cell Biol 13*:2835–2845.

Doye V, Hurt EC. 1995. Genetic approaches to nuclear pore structure and function. *Trends Genet 11*:235–241.
Eichler DC, Craig N. 1994. Processing of eukaryotic ribosomal RNA. *Prog Nucleic Acid Res Mol Biol 49*:197–239.
Eisinger DP, Dick FA, Trumpower BL. 1997. Qrs1p, a 60S ribosomal subunit protein is required for joining of 40S and 60S subunits. *Mol Cell Biol 17*:5136–5145.
Elsdale TR, Fischberg M, Smith S. 1958. A mutation that reduces nucleolar number in *Xenopus laevis*. *Exp Cell Res 14*:642–643.
Fabre E, Boelens WC, Wimmer C, Mattaj IW, Hurt EC. 1994. Nup145p is required for nuclear export of mRNA and binds homopolymeric RNA in vitro via a novel conserved motif. *Cell 78*:275–289.
Frank D, Patterson B, Guthrie C. 1992. Synthetic lethal mutations suggest interactions between U5 small nuclear RNA and four proteins required for the second step of splicing. *Mol Cell Biol 12*:5197–5205.
Fuller-Pace FV. 1994. RNA helicases: Modulators of RNA structure. *Trends Cell Biol 4*:271–274.
Gadal O, Strauss D, Braspenning J, Hoepfner D, Petfalski E, Philippsen P, Tollervey D, Hurt E. 2001. A nuclear AAA-type ATPase (Rix7p) is required for biogenesis and nuclear export of 60S ribosomal subunits. *EMBO J 20*:3695–3704.
Gaiano N, Amsterdam A, Kawakami K, Allende M, Becker T, Hopkins N. 1996. Insertional mutagenesis and rapid cloning of essential genes in zebrafish. *Nature 383*:829–832.
Giordano E, Peluso I, Senger S, Furia M. 1999. *minifly*, a *Drosophila* gene required for ribosome biogenesis. *J Cell Biol 144*:1123–1133.
Harnpicharnchai P, Jakovljevic J, Horsey E, Miles T, Roman J, Rout M, Meagher D, Imai B, Guo Y, Brame CJ, Shabanowitz J, Hunt DF, Woolford JL Jr. 2001. Composition and functional characterization of yeast 66S ribosome assembly intermediates. *Mol Cell 8*:505–515.
Helser T, Baan R, Dahlberg A. 1981. Characterization of a 40S ribosomal subunit complex in polyribosomes of *Saccharomyces cerevisiae* treated with cycloheximide. *Mol Cell Biol 1*:51–57.
Ho JH-N, Johnson AW. 1999. *NMD3* encodes an essential cytoplasmic protein required for stable 60S ribosomal subunits in *Saccharomyces cerevisiae. Mol Cell Biol 19*:2389–2399.
Hong B, Brockenbrough JS, Wu P, Aris JP. 1997. Nop2p is required for pre-rRNA processing and 60S ribosome subunit synthesis in yeast. *Mol Cell Biol 17*:378–388.
Ito H, Fukuda Y, Murata K, Kimura A. 1983. Transformation of intact yeast cells treated with alkali cations. *J Bacteriol 153*:163–168.
Kang HA, Hershey JW. 1994. Effect of initiation factor eIF-5A depletion on protein synthesis and proliferation of *Saccharomyces cerevisiae*. *J Biol Chem 269*:3934–3940.
Kay MA, Jacobs-Lorena M. 1985. Selective transitional regulation of ribosomal protein gene expression during early development of *Drosophila melanogaster*. *Mol Cell Biol 5*:3583–3592.
Koonin EV, Altschul SF, Bork P. 1996. Functional motifs. *Nature Genet 13*:266–267.
Kressler D, de la Cruz J, Rojo M, Linder P. 1998. Dbp6p is an essential putative ATP-dependent RNA helicase required for 60S-ribosomal-subunit assembly in *Saccharomyces cerevisiae*. *Mol Cell Biol 18*:1855–1865.
Kressler D, Linder P, de la Cruz J. 1999. Protein *trans*-acting factors involved in ribosome biogenesis in *Saccharomyces cerevisiae. Mol Cell Biol 19*:7897–7912.
Liao XC, Tang J, Rosbash M. 1993. An enhancer screen identifies a gene that encodes the yeast U1 snRNP A protein: Implications for snRNP protein function in pre-mRNA splicing. *Genes & Dev 7*:419–428.
Margossian SP, Li H, Zassenhaus HP, Butow RA. 1996. The DexH box protein Suv3p is a component of a yeast mitochondrial 3′-to-5′ exoribonuclease that suppresses group I intron toxicity. *Cell 84*:199–209.
Mitchell P, Petfalski E, Shevchenko A, Mann M, Tollervey D. 1997. The exosome: A conserved eukaryotic RNA processing complex containing multiple 3′ → 5′ exoribonucleases. *Cell 91*:457–466.
Moritz M, Paulovich AG, Tsay YF, Woolford JL Jr. 1990. Depletion of yeast ribosomal proteins L16 and rp59 disrupt ribosomal assembly. *J Cell Biol 111*:2261–2274.
Moritz M, Pulaski BA, Woolford JL Jr. 1991. Assembly of 60S ribosomal subunits is perturbed in temperature-sensitive yeast mutants defective in ribosomal protein L16. *Mol Cell Biol 11*:5681–5692.
Pause A, Méthot N, Sonenberg N. 1993. The HRIGRXXR region of the DEAD box RNA helicase eukaryotic translation initiation factor 4A is required for RNA binding and ATP hydrolysis. *Mol Cell Biol 13*:6789–6798.
Pause A, Sonenberg N. 1992. Mutational analysis of a DEAD box RNA helicase: The mammalian translation initiation factor eIF-4A. *EMBO J 11*:2643–2654.
Pierandrei-Amaldi P, Beccari E, Bozzoni I, Amaldi F. 1985. Ribosomal protein production in normal and anucleolate *Xenopus* embryos: Regulation at the posttranscriptional and translational levels. *Cell 42*:317–323.
Pringle J, Preston RA, Adams AE, Stearns T, Drubin DG, Haarer BK, Jones EW. 1989. Fluorescence microscopy methods for yeast. *Methods Cell Biol 31*:357–435.
Procunier JD, Tartof KD. 1975. Genetic analysis of the 5S RNA genes in *Drosophila melanogaster*. *Genetics 81*:515–523.
Ripmaster TL, Vaughn GP, Woolford JL Jr. 1992. A putative ATP-dependent RNA helicase involved in *Saccharomyces cerevisiae* ribosome assembly. *Proc Natl Acad Sci USA 89*:11131–11135.
Ripmaster TL, Vaughn GP, Woolford JL Jr. 1993. *DRS1* to *DRS7*, novel genes required for ribosome assembly and function in *Saccharomyces cerevisiae. Mol Cell Biol 13*:7901–7912.
Rotenberg MO, Moritz M, Woolford JL Jr. 1988. Depletion of *Saccharomyces cerevisiae* ribosomal protein L16 causes a decrease in 60S ribosomal subunits and formation of half-mer polyribosomes. *Genes & Dev 2*:160–172.
Sambrook J, Fritsch EF, Maniatis T. 1989. *Molecular cloning: A laboratory manual*. Cold Spring Harbor, New York: Cold Spring Harbor Laboratory Press.
Schwer B. 2001. A new twist on RNA helicases: DExH/D box proteins as RNPases. *Nat Struct Biol 8*:113–116.
Sherman F, Fink GR, Hicks JB. 1986. *Methods in yeast genetics*. Cold Spring Harbor, New York: Cold Spring Harbor Laboratory Press.
Simos G, Segref A, Fasiolo F, Hellmuth K, Shevchenko A, Mann M, Hurt EC. 1996. The yeast protein Arc1p binds to tRNA and functions as a cofactor for the methionyl- and glutamyl-tRNA synthetases. *EMBO J 15*:5437–5448.
Stage-Zimmermann T, Schmidt U, Silver PA. 2000. Factors affecting nuclear export of the 60S ribosomal subunit in vivo. *Mol Biol Cell 11*:3777–3789.
Sun C, Woolford JL Jr. 1994. The yeast *NOP4* gene product is an essential nucleolar protein required for pre-rRNA processing and accumulation of 60S ribosomal subunits. *EMBO J 13*:3127–3135.
Tanner NK, Linder P. 2001. DExD/H Box RNA heicase: From generic motors to specific dissociation functions. *Mol Cell 8*:251–262.
Vanzo NF, Li YS, Py B, Blum E, Higgins CF, Raynal LC, Krisch HM, Carpousis AG. 1998. Ribonuclease E organizes the protein interactions in the *Escherichia coli* degradosome. *Genes & Dev 12*:2270–2281.
Venema J, Bousquet-Antonelli C, Gelugne JP, Caizergues-Ferrer M, Tollervey D. 1997. Rok1p is a putative RNA helicase required for rRNA processing. *Mol Cell Biol 17*:3398–3407.
Venema J, Planta RJ, Raué HA. 1998. *In vivo* mutational analysis of ribosomal RNA in *Saccharomyces cerevisiae*. In: Martin R, ed. *Protein synthesis: Methods and protocols*. Totowa, New Jersey: Humana Press.
Venema J, Tollervey D. 1996. *RRP5* is required for formation of both 18S and 5.8S rRNA in yeast. *EMBO J 15*:2701–2714.
Venema J, Tollervey D. 1999. Ribosome synthesis in *Saccharomyces cerevisiae*. *Annu Rev Genet 33*:261–311.
Vilardell J, Warner JR. 1997. Ribosomal protein L32 of *Saccharomyces cerevisiae* influences both the splicing of its own transcript and the processing of rRNA. *Mol Cell Biol 17*:1959–1965.
Wallace H, Birnstiel ML. 1966. Ribosomal cistrons and the nucleolar organizer. *Biochim Biophys Acta 114*:296–310.
Warner JR. 1999. The economics of ribosome biosynthesis in yeast. *Trends Biochem Sci 24*:437–440.
Weaver PL, Sun C, Chang TH. 1997. Dbp3p, a putative RNA helicase in *Saccharomyces cerevisiae*, is required for efficient pre-

rRNA processing predominantly at site A_3. *Mol Cell Biol 17*:1354–1365.

Xu D, Field D, Tang SJ, Moris A, Bobechko B, Friesen J. 1998. Synthetic lethality of yeast *slt* mutations with U2 nuclear RNA mutations suggests functional interactions between U2 and U5 snRNPs that are important for both steps of pre-mRNA splicing. *Mol Cell Biol 18*:2055–2066.

Zanchin NIT, Roberts P, de Silva A, Sherman F, Goldfarb DS. 1997. *Saccharomyces cerevisiae* Nip7p is required for efficient 60S ribosome subunit biogenesis. *Mol Cell Biol 17*:5001–5015.

Zhang X, Moréra S, Bates PA, Whitehead PC, Coffer AI, Hainbucher K, Nash RA, Sternberg MJE, Lindahl T, Freemont PS. 1998. Structure of an XRCC1 BRCT domain: A new protein-protein interaction module. *EMBO J 17*:6404–6411.